

Synthesis, Characterization AC Electrical Properties of Cd Doped with Nano Nickel Ferrite by Sol -Gel

Malik Jabbar*, Farah T.M.Noori⁺, Abdulhadi.Kadhimi*

*Laser and optoelectronic Eng. Department, University of Technology, Baghdad, Iraq;

⁺College of science, Physics department, university of Baghdad, Baghdad, Iraq;

Abstract: Cadmium doping with nickel ferrite with general formula $Cd_xNi_{1-x}Fe_2O_4$ ($x = 0.0, 0.1, 0.3, 0.5$ and 0.7) has been prepared by using Sol-Gel method. The X-ray spectra shown indicate formation of crystalline cubic spinel phase ferrite, with appearance of small amount of secondary phases. The lattice parameter results were $8.38^{\circ}A - 8.446^{\circ}A$. Surface morphology features were studied by AFM and SEM. The dielectric measurement of the samples at room temperature studied in the frequency range 10 Hz to 5MHz shows dispersion in the low frequency region and remains constant at high frequency region. However, the small polar hopping type of conduction mechanism was inferred from the linear increase of AC conductivity. It is also found that dielectric constant increases with cadmium content increasing while it decreases with decrease of cadmium content.

I. Introduction

Ferrites nanoparticles are of great interest because of their scientific aspect and several applications. The Nano ferrites are interesting materials owing to their wide range of applications in new science and technology [1]. Cadmium substituted nickel ferrites are the important class of spinel ferrites [2]. According to crystal structure, nickel ferrite is an inverse spinel ferrite and possesses high electrical resistivity and low eddy current losses [3]. They are attractive because of their numerous specialized applications importance in Ferro fluids, magnetic drug delivery, Nano gadgets, sensors and hyper thermic for cancer treatment [4]. The structural and magnetic properties of spinel ferrites depend on the magnetic interaction and cation distribution in the two sub-lattices *i.e.* tetrahedral (A) and octahedral (B) lattice sites [5]. Cd substituted Ni ferrite nanoparticles were prepared by sol-gel method. In this search, the effect of Cd^{2+} substitution in $NiFe_2O_4$ is studied. The sol-gel method is used to synthesize the nanoparticles of $Cd_xNi_{1-x}Fe_2O_4$. The structural and AC electrical properties of the synthesized samples have been discussed in the contents.

1.2 Experimental Details

The Nano-ferrites of the composition $Cd_xNi_{1-x}Fe_2O_4$ (where $x = 0.0, 0.1, 0.3, 0.5$ and 0.7) were prepared by Sol-gel method by the below mentioned raw materials. The Nickel nitrate -99% Pure (AR Grade) $Ni(NO_3)_2$, Cadmium nitrate -99% Pure (AR Grade) $Cd(NO_3)_2$ and Iron nitrate -99% Pure (AR Grade) $Fe_2(NO_3)_2$ were dissolved in 50 ml from methanol and 50 ml from the distilled water, all these are collected in glass beaker and mixed well at room temperatures by hot plate magnetic stirrers with high speed, Ammonia solution was added slowly the form of drops into the mixed solution to control its pH until reach threats from 7 to 10 with continuous rotation. Gradually increase in temperature to reaches of $60^{\circ}C$ and continues the solution to this heats for one hours. After the completion of the solution turned to gel, the temperature drops to the room temperature and this gel become dry and dark browns and then place it in an oven at a temperature of $150^{\circ}C$ for a three hours then it will become dry gel. The powder was pressed using a die with diameter (1.5cm) to produce specimens in a pellet shapes. The pressing load used was (3 ton) and the specimens held for 10 min under pressure using a hydraulic press of a maximum load 10 ton.

II. Results and Discussion

2.1 X-Ray Diffraction Results:

The XRD patterns of the $(Cd_xNi_{1-x}Fe_2O_4)$ bulk is shown in Figure (1). The X-ray diffraction appearance of all samples the single phase of cubic spinel structure which agrees with result of [6]. The existence of Miller indices conforms (202), (313) and (400) major lattice plane and uncovers the cubic spinel phases that is specified by the reference of powders diffraction files as shown in Table 1 [7]. Additionally, secondary lattice planes of (111), (200), (333) and (531) were found. The peaks appeared different amounts of crystallinity depending upon concentration rates of Cd^{+} . The Miller indices (hkl), d-spacing (d_{hkl}) and the lattice parameters are listed in Tables (1) and (2). All XRD measurements revealed match well with the typical patterns of inverse spinel ferrite. Interplanar distance and planes are calculated by Bragg's diffraction law and index method using equation 1 and 2 [8]. The X-ray density depends on the lattice parameters and molecular weights of the samples and the values increase with increasing of Cd content, while particles size decreases with increasing of Cd

content. The average crystallite size has been calculated from the full width at half maximum of the reflection and using the Scherer's formula equation 3 [9].

$$n\lambda = 2d \sin \theta \tag{1}$$

The lattice parameter 'a' was determined using following relation

$$a = d \times \sqrt{h^2 + k^2 + l^2} \tag{2}$$

Scherer's formula is
$$D = \frac{0.9\lambda}{\beta \cos \theta} \tag{3}$$

where *D* is the crystallite size, β is the full width of the diffraction line at half of the maximum intensity measured in radians, λ is x-ray wavelength (Cu α radiation, 1.5405Å) and θ is the Bragg angle.

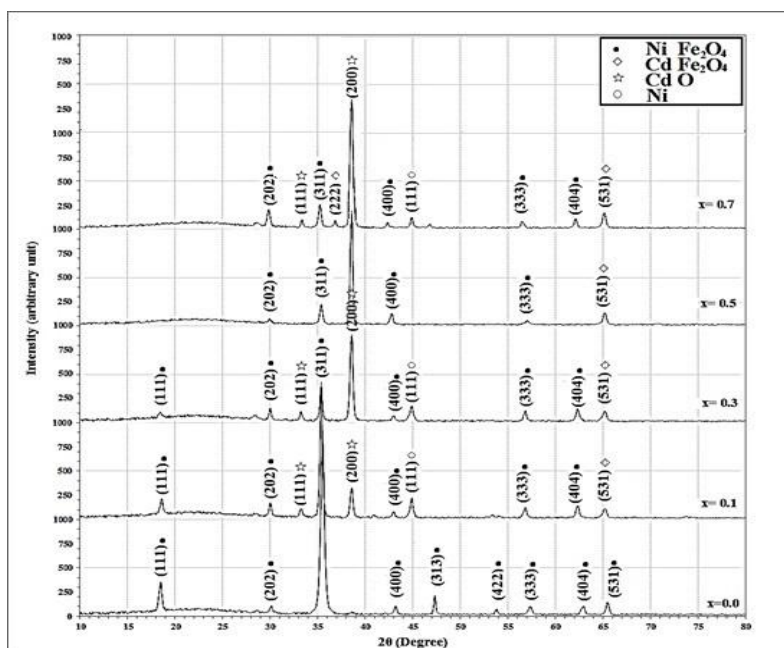


Figure 1: XRD spectral data for (Cd_xNi_{1-x}Fe₂O₄) nanocomposite with different concentrations of Cd.

Table 1: XRD spectra data for (Cd_xNi_{1-x}Fe₂O₄) nanocomposite with different concentrations of Cd.

Cd content	2θ (Deg.)	FWHM (Deg.)	d _{hkl} Exp.(Å)	G.S (nm)	hkl	d _{hkl} Std.(Å)	Phase	Card No.
0.0	18.4500	0.2859	4.8050	28.2	(111)	4.8265	NiFe ₂ O ₄	96-230-0296
	30.1215	0.2859	2.9645	28.8	(202)	2.9556	NiFe ₂ O ₄	96-230-0296
	35.4968	0.4575	2.5269	18.2	(311)	2.5205	NiFe ₂ O ₄	96-230-0296
	43.1594	0.3431	2.0944	24.9	(400)	2.0899	NiFe ₂ O ₄	96-230-0296
	47.3000	0.2287	1.9202	37.9	(313)	1.9178	NiFe ₂ O ₄	96-230-0296
	53.7956	0.2859	1.7027	31.2	(422)	1.7064	NiFe ₂ O ₄	96-230-0296
	57.3410	0.4575	1.6056	19.8	(333)	1.6088	NiFe ₂ O ₄	96-230-0296
	62.8878	0.3431	1.4766	27.1	(404)	1.4778	NiFe ₂ O ₄	96-230-0296
	66.1000	0.4003	1.4124	23.7	(531)	1.4130	NiFe ₂ O ₄	96-230-0296
	18.5500	0.3240	4.7793	24.9	(111)	4.8265	NiFe ₂ O ₄	96-230-0296
0.1	30.0254	0.2861	2.9737	28.8	(202)	2.9556	NiFe ₂ O ₄	96-230-0296
	33.2295	0.3433	2.6940	24.2	(111)	2.7032	CdO	96-900-6675
	35.3465	0.2861	2.5373	29.2	(311)	2.5205	NiFe ₂ O ₄	96-230-0296
	38.5505	0.2861	2.3335	29.4	(200)	2.3410	CdO	96-900-6675
	42.9561	0.2861	2.1038	29.9	(400)	2.0899	NiFe ₂ O ₄	96-230-0296
	44.8442	0.3433	2.0195	25.0	(111)	2.0201	Ni	96-901-1604
	56.8023	0.3433	1.6195	26.3	(333)	1.6088	NiFe ₂ O ₄	96-230-0296
	62.3522	0.4005	1.4880	23.2	(404)	1.4778	NiFe ₂ O ₄	96-230-0296
	65.1558	0.4577	1.4306	20.6	(531)	1.4283	CdFe ₂ O ₄	96-591-0006
	18.4340	0.3210	4.8091	25.1	(111)	4.8265	NiFe ₂ O ₄	96-230-0296
30.0143	0.2289	2.9748	35.9	(202)	2.9556	NiFe ₂ O ₄	96-230-0296	

0.3	33.2189	0.2861	2.6948	29.0	(111)	2.7032	CdO	96-900-6675
	35.3362	0.2861	2.5380	29.2	(311)	2.5205	NiFe ₂ O ₄	96-230-0296
	38.5408	0.2861	2.3341	29.4	(200)	2.3410	CdO	96-900-6675
	42.9471	0.3433	2.1042	24.9	(400)	2.0899	NiFe ₂ O ₄	96-230-0296
	44.8355	0.4006	2.0199	21.5	(111)	2.0201	Ni	96-901-1604
	56.7954	0.2861	1.6197	31.6	(333)	1.6088	NiFe ₂ O ₄	96-230-0296
	62.3462	0.4006	1.4881	23.2	(404)	1.4778	NiFe ₂ O ₄	96-230-0296
0.5	65.1502	0.4578	1.4307	20.6	(531)	1.4283	CdFe ₂ O ₄	96-591-0006
	29.9760	0.3433	2.9785	24.0	(202)	2.9556	NiFe ₂ O ₄	96-230-0296
	35.3500	0.3433	2.5361	24.3	(311)	2.5205	NiFe ₂ O ₄	96-230-0296
	38.5408	0.2289	2.3341	36.8	(200)	2.3410	CdO	96-900-6675
	42.7430	0.2861	2.1138	29.8	(400)	2.0899	NiFe ₂ O ₄	96-230-0296
	57.0243	0.4006	1.6137	22.6	(333)	1.6088	NiFe ₂ O ₄	96-230-0296
	65.1502	0.4006	1.4307	23.5	(531)	1.4283	CdFe ₂ O ₄	96-591-0006
	33.3366	0.2289	2.6856	36.2	(111)	2.7032	CdO	96-900-6675
	35.2110	0.3428	2.5468	24.3	(311)	2.5205	NiFe ₂ O ₄	96-230-0296
	36.8270	0.2290	2.4386	36.6	(222)	2.4393	CdFe ₂ O ₄	96-591-0006
	38.5961	0.2290	2.3308	36.8	(200)	2.3410	CdO	96-900-6675
0.7	42.3781	0.2860	2.1312	29.8	(400)	2.0899	NiFe ₂ O ₄	96-230-0296
	44.8502	0.2859	2.0193	30.1	(111)	2.0201	Ni	96-901-1604
	46.7273	0.2866	1.9424	30.2	(313)	1.9178	NiFe ₂ O ₄	96-230-0296
	56.5300	0.2864	1.6266	31.5	(333)	1.6088	NiFe ₂ O ₄	96-230-0296
	62.1320	0.3433	1.4928	27.0	(404)	1.4778	NiFe ₂ O ₄	96-230-0296
	65.0989	0.4005	1.4317	23.5	(531)	1.4283	CdFe ₂ O ₄	96-591-0006

Table2: XRD spectra data for Cd_xNi_{1-x}Fe₂O₄ ferrites at the plane (311).

X	d _{hkl} (°A)	hkl	M(g/mol)	a (°A)	V(cm ³)	dx(g/cm ³)
0.0	2.5269	(311)	234.38	8.380	5.89*10 ⁻²²	5.289
0.1	2.5373	(311)	239.75	8.415	5.96*10 ⁻²²	5.344
0.3	2.538	(311)	250.49	8.417	5.96*10 ⁻²²	5.579
0.5	2.5361	(311)	261.23	8.411	5.96*10 ⁻²²	5.831
0.7	2.5468	(311)	271.98	8.446	6.03*10 ⁻²²	5.995

2.2 Atomic Force Microscopy (AFM) results:

Figures 2 show the atomic forces microscopy images of bulk Cd_xNi_{1-x}Fe₂O₄ ferrites where (x=0.0,0.1,0.3,0.5 and 0.7). The AFM images of all samples show granular structure. The average grain size and average roughness as determined from atomic force microscopy are given in Table (3). Both the average grain size and average roughness increase with the increases in Cd substitution, that mean increases in the power of bond of linking atoms this agrees with the result of references [10]. Though the averages grain size of (x=0.0) and (0.7) increase from 63.50nm to 83.16 nm respectively as shown in figure2. On the other hand, the averages roughness increases from 1.69 to 4.42nm when x increased from 0.0 to 0.7.

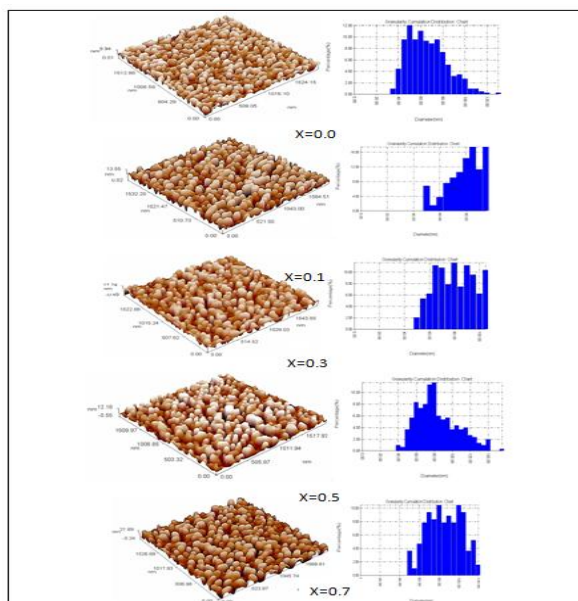


Figure 2: The AFM images of Cd_xNi_{1-x}Fe₂O₄ for different cadmium concentrations at (x=0.0,0.1,0.3,0.5 and 0.7).

Table 3: Average grain size and average roughness for $Cd_xNi_{1-x}Fe_2O_4$ where ($x=0, 0.1, 0.3, 0.5$ and 0.7)

Cd content	Ave. grain size (nm)	Ave. Roughness (nm)
0.0	63.50	1.69
0.1	76.45	2.97
0.3	77.86	3.81
0.5	81.32	3.23
0.7	83.16	4.42

2.3 Scanning Electron Microscopy (SEM)

Figure 3 shows the SEM micrograph images for bulk $Cd_xNi_{1-x}Fe_2O_4$ where ($x=0.0, 0.1, 0.3, 0.5$ and 0.7). The SEM image show that the samples are not closely packed and consist of several grains and agree with [11]. The cadmium additions showed no major effect on the surface morphology of the ferrites.

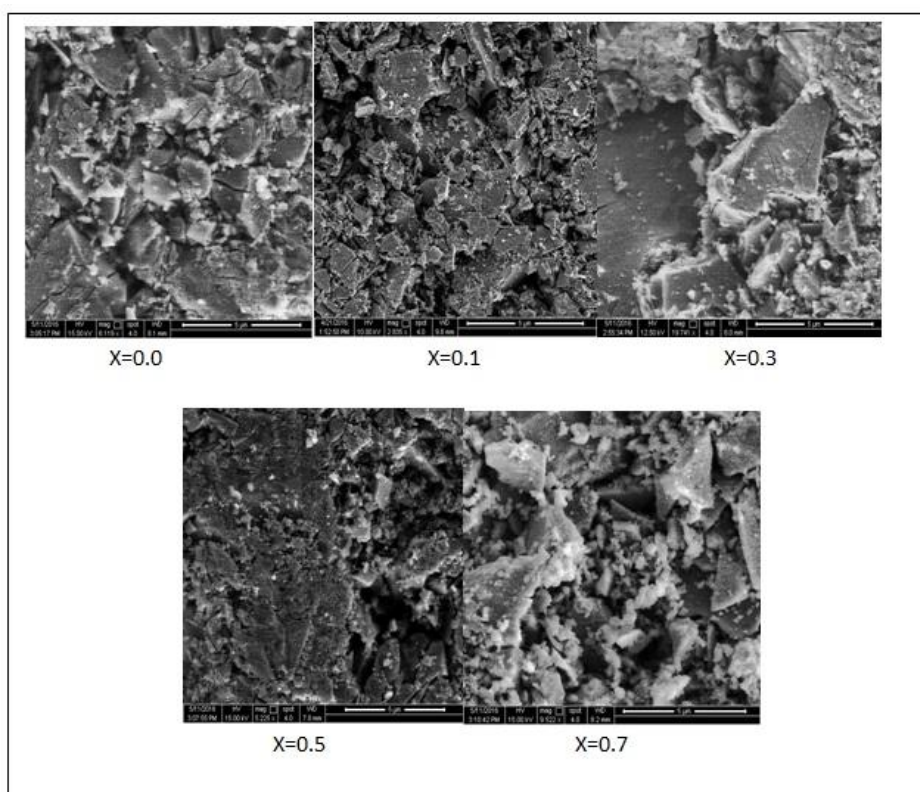


Figure3 : SEM images for $Cd_xNi_{1-x}Fe_2O_4$ bulk at different cadmium concentrations at ($x=0.0, 0.1, 0.3, 0.5$ and 0.7).

2.4 Electrical Properties

The electrical properties of cadmium doped nickel ferrite $Cd_xNi_{1-x}Fe_2O_4$ include the A.C conductivity and dielectric properties.

2.4.1 The AC Electrical Properties of Bulk

The variation of A.C electrical conductivity of bulk $Cd_xNi_{1-x}Fe_2O_4$ with frequency is shown in figure 4. It Can be noted the A.C conductivity $\sigma_{ac}(\omega)$ increases with increase in the frequency for all specimens. Which is the normal behavior of ferrites this agrees with the result of references [12]. As mentioned above the conduction in ferrites mainly due to exchange of electrons amongst Fe^{3+} and Fe^{2+} ions. The boost in frequency of the connected field expands the bouncing of charges bearers bringing about increase in conductivity and lessening of resistivity. Typical conduct of ferrites is the ordinary conduct of ferrites. ItCan be observed that AC conductivity increase with increase with increase in cadmium content in nickel ferrite.

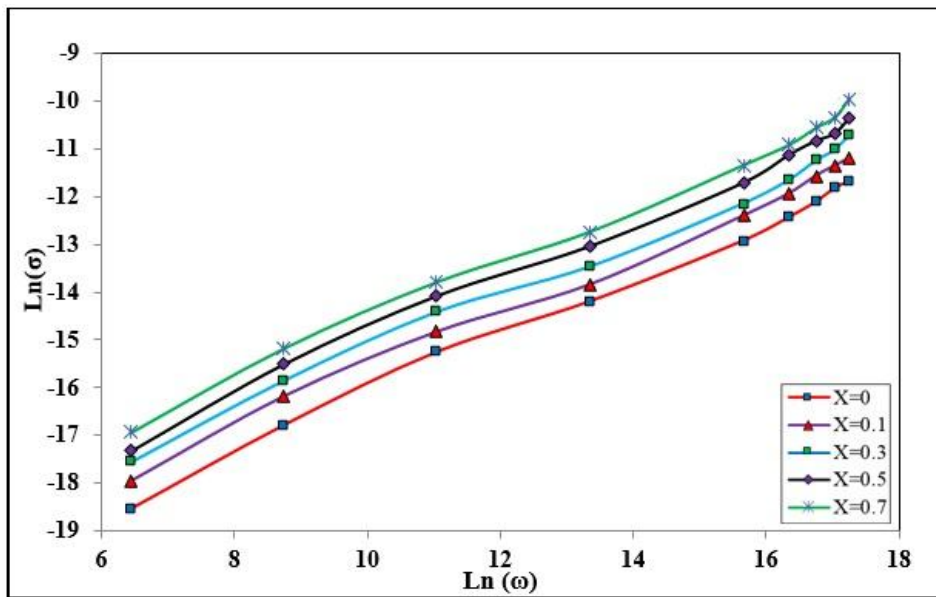


Figure 4: A.C electrical conductivity as a function of frequency for $Cd_xNi_{1-x}Fe_2O_4$ with different contents of Cd.

2.4.2 The Dielectric Constant of Bulk

Figures 5 and 6 show the dependence of the real and imaginary part of dielectric constant ϵ_1 , ϵ_2 for bulk $Cd_xNi_{1-x}Fe_2O_4$ on the frequency ω , for different cadmium doping contents. The real and imaginary part of dielectric constant for all samples decrease with increasing of frequency. This behavior agrees well with Deby's type relaxation process. The real and imaginary part of dielectric constant reach a constant value for all the samples above certain greater frequency, this agrees with the result of references [13,14]. It can be observed from Figure 6 that the imaginary part of dielectric constant ϵ_2 increases with frequency. The imaginary part of dielectric constant ϵ_2 refers to the dielectric loss.

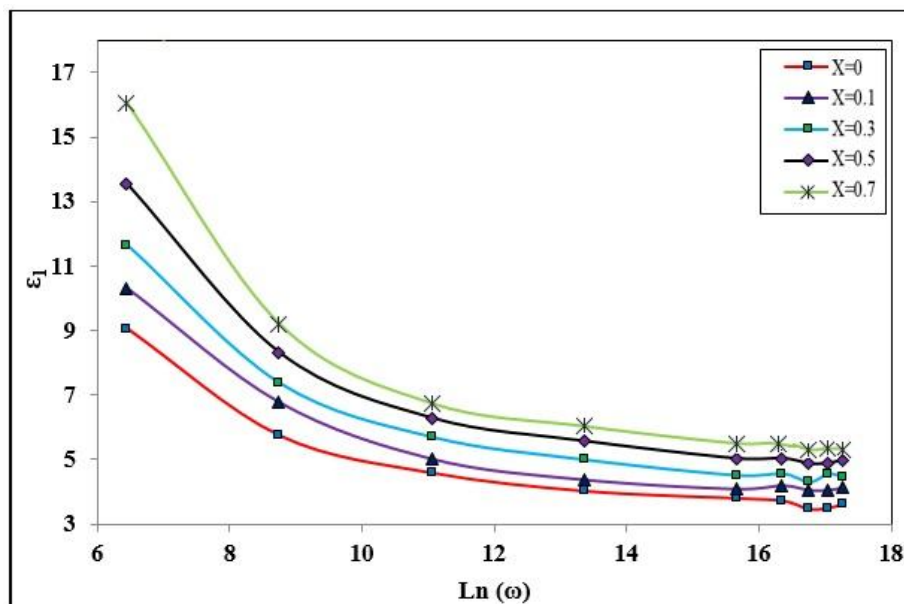


Figure 5: Variation of real part (ϵ_1) of dielectric constant with frequency for $Cd_xNi_{1-x}Fe_2O_4$ at different Cd contents.

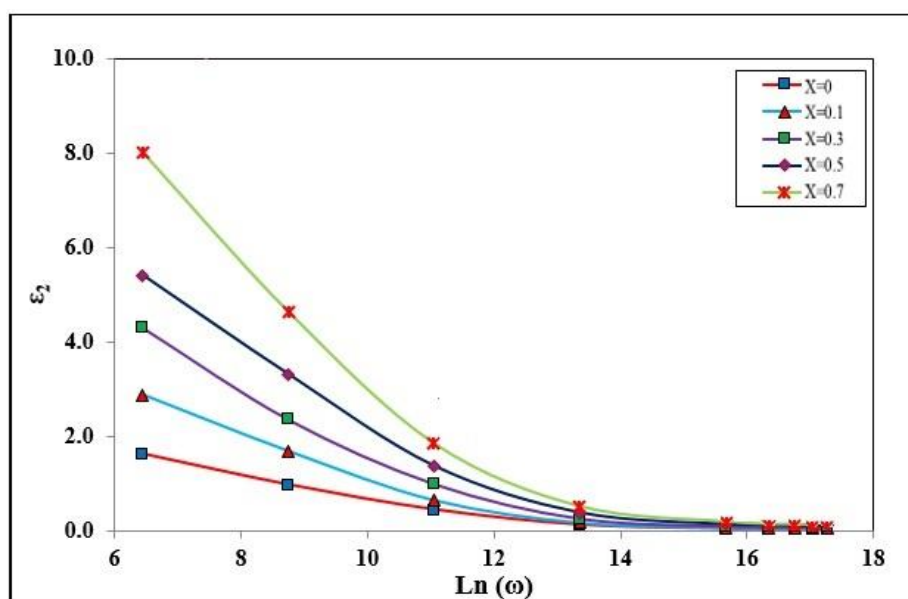


Figure 6: Variation of imaginary part (ϵ_2) of dielectric constant with frequency for $\text{Cd}_x\text{Ni}_{1-x}\text{Fe}_2\text{O}_4$ at different Cd contents.

III. Conclusion

The $\text{Cd}_x\text{Ni}_{1-x}\text{Fe}_2\text{O}_4$ where ($x= 0.0,0.1,0.3,0.5$ and 0.7) Nano ferrites were prepared using Sol-Gel method. The X-ray diffraction studies clearly showed formations of the crystalline structure of $(\text{Cd}_x\text{Ni}_{1-x}\text{Fe}_2\text{O}_4)$ is cubic spinel structure phase ferrite and the particle size beyond the nanoscale. The lattice parameter is found to increase with increasing cadmium content. AFM results show clearly that the average roughness of $(\text{Cd}_x\text{Ni}_{1-x}\text{Fe}_2\text{O}_4)$ increases with increasing cadmium contents. The real and imaginary part of dielectric constant decrease with increasing of frequency, while the A.C electrical conductivity is increased with increasing of frequency.

Reference

- [1]. Q. Song, Q. Zhang and Z. John, Shape Control and Associated Magnetic Properties of Spinel Cobalt Ferrite Nanocrystals". *Journal of the American Chemical Society*, 126, 2004, 6164-6168.
- [2]. S. E. Shirsath, B. G. Toksha and K. M. Jadhav, Structural and Magnetic Properties of In^{3+} Substituted NiFe_2O_4 , *J. Materials Chemistry and Physics*, 117(1), 2009, 163-168.
- [3]. M. Mozaffari, J. Amighian, E. Darsheshdar, Magnetic and structural studies of Nickel – substituted cobalt ferrite nanoparticles, synthesized by sol-gel method' *Journal of Magnetism and Magnetic materials*, 350, 2014, 19-22.
- [4]. A. Goldman, Modern Ferrite Technology, (Van Nostrand Reinhold, New York, 1990).
- [5]. S. Manjura Hoque, Md. Amanullah Choudhury and Md. Fakhrul Islam, Characterization of Ni-Cu Mixed Spinel Ferrite, *Journal of Magnetism and Magnetic Materials*, 251(3), 2002, 292-303.
- [6]. M. Siva Ram Prasad, B.B.V.S.V. Prasad, B. Rajesh b, K.H. Rao and K.V. Ramesh, "Magnetic Properties and Dc Electrical Resistivity Studies On Cadmium Substituted Nickel–Zinc Ferrite System", *Journal of Magnetism and Magnetic Materials*, 323, 2011, 2115–2121.
- [7]. (card no. 96-230-0296) from (ICDD) International Centre for Diffraction Data.
- [8]. G. R. Kumar, K. V. Kumar and Y. C. Venudhar, Synthesis, Structural and Magnetic Properties of Copper Substituted Nickel Ferrites by Sol-Gel Method, *J. Materials Sciences and Applications*, 3, 2012, 87-91.
- [9]. G. Nabiyouni, M. Jafari Fesharaki, M. Mozafari and J. Amighian, Characterization and Magnetic Properties of Nickel Ferrite Nanoparticles Prepared by Ball Milling Technique, *Chin. Phys. Lett.*, 27(12), 2010, 6401.
- [10]. M.K. Khalaf, N. A. Al-Tememe, F.T. Ibrahim and M. A. Hameed, Crystalline Structure and Surface Morphology of Tin Oxide Films Grown by DC Reactive Sputtering, *Photonic Sensors*, 4(4), 2014, 349–353.
- [11]. S. Ghatak, G. Chakraborty, Sinha, S. Pradhan, and A. K. Meikap, Direct and Alternate Current Conductivity and Magneto conductivity of Nano crystalline Cadmium-Zinc Ferrite below Room Temperature, *J. Materials Sciences and Applications*, 2, 2011, 226-236.
- [12]. P.A. Noorkhan and S. Kalayne, "Synthesis, Characterization Ac Conductivity of Nickel Ferrite", *Journal of Engineering Research and Applications*, 2, 2012, 681-685.
- [13]. S. Yanez-Vilar, M. Sanchez, C. Gomez-Aguirre, J. Mira, M.A. Senaris-Rodriguez and S. Castro-Garcia, A simple solvothermal Synthesis of MFe_2O_4 ($\text{M} = \text{Mn}, \text{Co}$ and Ni) Nanoparticles, *Journal of Solid State Chemistry*, 182, 2009, 2685–2690.
- [14]. R. S. Devan, Y. D. Kolekar and B. K. Coagula, "Effect Of Cobalt Substitution on The Properties of Nickel–Copper Ferrite", *J. Physics: Condensed Matter*, 18, 2006, 43.